Letter

Black hole ringdown spectroscopy of curvature-coupled scalar and pseudoscalar fields

Adrian Ka-Wai Chung[1,2,*] and Nicolás Yunes[2]

[1]DAMTP, Centre for Mathematical Sciences, University of Cambridge, Wilberforce Road, Cambridge CB3 0WA, United Kingdom

[2]Illinois Center for Advanced Studies of the Universe and Department of Physics, University of Illinois Urbana-Champaign, Urbana, Illinois 61801, USA

(Received 20 June 2025; accepted 12 June 2026; published 28 July 2026)

Remnant black holes formed in compact binary coalescences provide a clean setting for probing additional fields coupled to gravity. By analyzing the ringdown signals of the loudest LIGO-Virgo-KAGRA binary-black hole mergers, we search for massless curvature-coupled (pseudo)scalar fields arising in extensions to general relativity. We find no evidence for such fields and place 90% credible upper limits on the coupling length scale, $\ell \lesssim (25\text{–}45)$ km, corresponding to scales significantly below the horizons of the remnant black holes. These results include the first gravitational-wave constraint on an axidilaton-type coupling. By isolating the ringdown phase and performing extensive robustness checks, our analysis provides a complementary observational probe to existing full-waveform constraints. As the gravitational-wave catalog expands, black hole ringdown spectroscopy will enable increasingly sensitive probes of gravity and additional fields using astrophysical black holes.

DOI: 10.1103/2ctd-mgb6

Introduction. Additional fields coupled to gravity may help address several open questions in astronomy and fundamental physics, including the origin of cosmological inflation [1–3], the late-time acceleration of the Universe [4–6], matter-antimatter asymmetry [7,8], the nature of dark energy [9], and possible extensions to general relativity. Such fields can modify the spacetime surrounding astrophysical black holes [10–12], leading to deviations from the Kerr description predicted by general relativity. Binary black hole mergers observed through gravitational waves therefore provide a promising setting for searching for new fundamental fields [13–15], since these modifications can alter black hole dynamics and leave observable imprints on the emitted gravitational-wave signals [16,17].

The ringdown phase of binary black hole mergers provides a particularly promising setting for searching for curvature-coupled additional fields. During this phase, the newly formed black hole relaxes toward its final stationary state by emitting gravitational waves that can be described as a superposition of exponentially damped oscillations. The frequencies and decay times characterizing these quasinormal modes are determined primarily by the spacetime surrounding the remnant black hole and by the properties of the additional fields [18]. This relative simplicity, together with recent advances in black hole spectroscopy and gravitational-wave data analysis [19], has made ringdown observations an increasingly important tool for probing strong-field gravity.

In this work, we search for curvature-coupled (pseudo) scalar fields using recently computed quasinormal-mode spectra of black holes interacting with these fields [18,20–22] together with black hole ringdown signals detected by the LIGO-Virgo-KAGRA detectors. We consider three representative couplings; axidilaton, dynamical Chern-Simons, and scalar Gauss-Bonnet couplings. These theories have been studied in a variety of contexts connected to inflationary cosmology [3], Baryon asymmetry [23], and extensions to general relativity. They also arise naturally in low-energy effective descriptions of high-energy gravity frameworks, including string theory [10,24,25] and loop quantum gravity [8].

Here, we analyze black hole ringdown signals detected by the LIGO-Virgo-KAGRA detectors to search for curvature-coupled (pseudo)scalar fields. Our analysis employs recently computed quasinormal-mode spectra calibrated for remnant black holes with dimensionless spin $a = |\vec{J}|/M^2 \in [0, 0.75]$, encompassing the spin range of most binary-black hole merger remnants observed to date. We also incorporate the parity-dependent shifts of quasinormal-mode spectra induced by these fields, which have not been explicitly

*Contact author: kwc43@cam.ac.uk

included in previous gravitational-wave searches. To assess the reliability of the inferred constraints, we investigate the impact of waveform-modeling and parameter-estimation systematics through a series of robustness tests. Finding no evidence for these fields, we place bounds on axidilaton, dynamical Chern-Simons, and scalar Gauss-Bonnet couplings, including the first gravitational-wave constraints on axidilaton-type coupling.

Models of (pseudo)scalar field. We consider two curvature-coupled (pseudo)scalar fields, φ_1 and φ_2, motivated by extensions to general relativity, high-energy gravity frameworks, and cosmology. In units with $c = G = 1$, which we adopt throughout this work, the fields satisfy

$$\Box\varphi_1 = -\ell_1{}^2\mathcal{G}, \qquad \Box\varphi_2 = -\ell_2{}^2\mathcal{P}. \tag{1}$$

Here $\Box$ is the wave operator, $\ell_{1,2}$ are coupling length scales with dimensions of length, $\mathcal{G} = R^2 - 4R_{\alpha\beta}R^{\alpha\beta} + R_{\alpha\beta\gamma\delta}R^{\alpha\beta\gamma\delta}$ is the Gauss-Bonnet invariant, and $\mathcal{P} = R_{\mu\nu\rho\sigma}\tilde{R}^{\mu\nu\rho\sigma}$ is the Pontryagin invariant, where $R_{\alpha\beta\gamma\delta}$, $R_{\alpha\beta}$, and R denote the Riemann tensor, Ricci tensor, and Ricci scalar, respectively, and $\tilde{R}^{\mu\nu\rho\sigma}$ is the dual Riemann tensor. The choice $(\ell_1, \ell_2) = (\ell, 0)$ corresponds to scalar Gauss-Bonnet coupling, while $(\ell_1, \ell_2) = (0, \ell)$ corresponds to dynamical Chern-Simons coupling. These couplings arise naturally in low-energy effective descriptions of string theory [10,24,25], while dynamical Chern-Simons gravity has also been studied in the context of loop quantum gravity [23] and baryon asymmetry [23]. The case $(\ell_1, \ell_2) = (\ell, \ell)$ describes axidilaton coupling, which has been explored in inflationary cosmology [3]. Additional details are provided in the Supplemental Material [26].

Coupling to these (pseudo)scalar fields deforms the black hole spacetime away from the Kerr solution, thereby shifting the quasinormal-mode spectrum of the remnant black hole. Existing gravitational-wave and astrophysical observations already constrain the coupling length scales $\ell_{1,2}$ to be small compared to the black hole mass M. In this small-coupling regime, the leading-order corrections to the spacetime and quasinormal-mode frequencies scale as $(\ell/M)^4$. The quasinormal-mode frequencies can then be expressed as

$$\omega^{(\mathrm{P})}(M, a, \ell_1, \ell_2) = \omega^{(0)}(M, a) + \zeta_1 \frac{\Omega_1^{(\mathrm{P})}(a)}{M} + \zeta_2 \frac{\Omega_2^{(\mathrm{P})}(a)}{M}, \tag{2}$$

where $\omega^{(0)}(M, a)$ denotes the quasinormal-mode frequency of a Kerr black hole with source-frame mass M and dimensionless spin a, while $\Omega_{1,2}^{(\mathrm{P})}(a)$ encode the leading-order parity (P)-dependent corrections induced by the couplings. We have introduced the dimensionless coupling parameters,

$$\zeta_{1,2} = \left[\frac{\ell_{1,2}(1+z)}{M_z}\right]^4, \tag{3}$$

where M_z and z are respectively the (redshifted) remnant mass and the redshift to the remnant black hole. For astrophysical black holes, $\omega^{(0)}(M, a)$ depends primarily on the remnant mass and spin[1] [28]. The functions $\Omega_{1,2}^{(\mathrm{P})}(a)$ for the dominant modes have been computed for spins $a \lesssim 0.75$ [18,21,22]. For axidilaton coupling, the corresponding corrections are given by the sum of the dynamical Chern-Simons and scalar Gauss-Bonnet contributions, as discussed in the Supplemental Material [26]. Throughout this work, we use the fitting expressions for $\Omega_{1,2}^{(\mathrm{P})}(a)$ provided in Refs. [18,21,22]. Although parameter estimation occasionally explores spins beyond $a = 0.75$, the inferred posteriors are dominated by the region within the calibrated spin range (see Supplemental Material [26]).

Data analysis.

Waveform model: The dependence of the quasinormal-mode spectra on the coupling length scales enables us to build a waveform model that describes the ringdown-phase gravitational waves emitted by black holes coupled to the additional fields [29],

$$h(t) = \frac{M_z}{d_L}\Theta(t - t_\mathrm{s}) \sum_{n,l,m,(\mathrm{P})} S_{nlm}(\iota, \phi) \times [A_{nlm}^{+,(\mathrm{P})} e^{-i\omega_{nlm}^{(\mathrm{P})}(t-t_\mathrm{s})} + A_{nlm}^{-,(\mathrm{P})} e^{+i(\omega_{nlm}^{(\mathrm{P})})^\dagger (t-t_\mathrm{s})}], \tag{4}$$

where $h = h_+ - ih_\times$, with $h_{+,\times}$ being the plus and cross-mode polarization of the gravitational waves respectively, $M_z = M(1+z)$ is the redshifted mass (i.e. the mass in the detector frame), d_L is the luminosity distance to the remnant black hole, $\sum_{n,\ell,m,(\mathrm{P})}$ stands for summation over $n \geq 0, l \geq 2, -l \leq m \leq l$, and parities ((P)), d_L is the luminosity distance to the remnant black hole, and $\Theta(t - t_s)$ is the Heaviside function that activates the waveform at the ringdown start time t_s. The quantity $S_{nlm}(\iota, \phi)$ are spin-weighted spheroidal harmonics, which are functions of the inclination angle ι between the remnant spin axis and the line of sight, and the azimuthal angle ϕ in the line of sight and in the source frame. The quantities $A_{nlm}^{+,(\mathrm{P})}$ and $A_{nlm}^{-,(\mathrm{P})}$ are complex mode amplitudes, where the superscript $+(-)$ stands for modes with a positive (negative) real-part frequency.

To simplify the analysis, we adopt two approximations. First, we assume $A_{nlm}^{N,q} = (-1)^l (A_{nlm}^{P,q})^\dagger$ [29,30]. This is a good approximation for nonprecessing binary-black hole mergers, and is consistent with the events analyzed here

[1] Strictly speaking, quasinormal-mode frequencies in general relativity can also depend on electric charge. However, astrophysical black holes are expected to neutralize rapidly through interactions with the surrounding plasma [27].

(see below), whose inferred remnant spins show no evidence for strong precession [31–33]. Second, we do not include scalar-led quasinormal modes associated with the additional fields in the present analysis. In the small-coupling regime explored here, these modes are expected to enter at higher order in the coupling parameters $\zeta_{1,2}$ and to remain subdominant within the sensitivity of current gravitational-wave observations. Our analysis therefore focuses on the leading-order modifications to the gravitational-sector quasinormal-mode spectrum induced by the curvature couplings.

Bayesian inference: The goal of this work is to search for the fields by measuring their coupling length scale ℓ using detected ringdown signals via Bayesian inference. To this end, We construct the marginalized posterior,

$$p(\ell|d,H,I) = \int d\vec{\theta}\, p(\ell,\vec{\theta}|d,H,I), \tag{5}$$

where $\vec{\theta}$ denotes other source parameters (e.g., M_z and d_L), d is the strain data, H is the hypothesis that the signal includes the additional-field effects, and I encodes prior knowledge, such as the quasinormal-mode spectra. By Bayes' theorem,

$$p(\ell,\vec{\theta}|d,H,I) = \frac{p(d|\ell,\vec{\theta},H,I)p(\ell,\vec{\theta}|H,I)}{p(d|H,I)}, \tag{6}$$

where $p(d|\ell,\vec{\theta},H,I)$ is the likelihood, $p(\ell,\vec{\theta}|H,I)$ is the prior, and $p(d|H,I)$ is the evidence. If multiple events are analysed, $d = \{d_i|i = 1,2,3,\ldots\}$, where d_i is the data of the ith event, the combined posterior is

$$p(\ell|d,H,I) \propto \prod_{i=1} p(\ell|d_i,H,I), \tag{7}$$

since ℓ is a coupling constant and the prior of ℓ is uniform (see below), which is the same in different events. The 90% credible upper limit ℓ_{90}, defined by

$$\int_0^{\ell_{90}} d\ell\, p(\ell|d,H,I) = 0.9, \tag{8}$$

gives us constraints on ℓ.

Parameter estimation: We analyze publicly available LIGO-Virgo-KAGRA data and focus on events satisfying two criteria; (i) a total signal-to-noise ratio $\gtrsim 25$, comparable to that of GW150914, and (ii) inclusion in previous ringdown-only tests of general relativity performed by the LIGO-Virgo-KAGRA Collaboration [30,34–36]. Applying these criteria, we analyze the ringdown phases of GW150914 [31], GW190521_074359 [37], GW200129_065458 [33], GW231226_101520, and GW250114_082203 [38]. The inferred progenitor spins of these events show no evidence for strong spin precession [32,33], consistent with the symmetry assumption $A^{-,(\mathrm{P})}_{nlm} = (-1)^l (A^{+,(\mathrm{P})}_{nlm})^\dagger$ adopted in Eq. (4).

Previous analyses of GW250114_082203 indicate the presence of an overtone contribution in the ringdown signal [38], and overtone signatures have also been discussed in earlier ringdown studies [39,40]. In the present analysis, we include only the dominant $nlm = 022$ mode for all events except GW250114_082203, for which we include both the 022 and 122 modes. For the overtone modes ($n = 1$), we assume vanishing coupling-induced corrections, i.e., $\Omega^{(\mathrm{P})}_{1,2}(a) \equiv 0$. This treatment is consistent with the fractional-deviation analyses of quasinormal-mode frequencies performed by the LIGO-Virgo-KAGRA Collaboration [30,38]. As shown in the robustness studies below, including overtone contributions does not significantly alter the inferred constraints.

We analyze the ringdown signals using pyRing [41], a Python package for time-domain black hole spectroscopy [42–44]. To reduce contamination from nonlinear dynamics during the early postmerger phase [45,46], the analysis begins at a time $10M_z$ after the peak of the strain amplitude [44]. The peak time and remnant mass M_z are estimated *a priori* from full-signal analyses assuming general relativity and are available in the public data releases accompanying each event [30,35]. Following standard procedures in black hole spectroscopy [29,30,35], we fix the sky location and inclination angle to the maximum-likelihood values inferred from full-signal parameter estimation. This approximation is justified because these extrinsic parameters are only weakly correlated with the coupling parameters inferred from the ringdown spectrum. We prescribe a uniform prior on the following parameters, following [29] [$M_z \in [10, 500] M_\odot$, $a \in [0, 0.93]$, $|A^{\pm,(\mathrm{P})}_{nlm}| \in [0, 50]$, and $\phi^{\pm,(\mathrm{P})}_{nlm} = \arg(A^{\pm,(\mathrm{P})}_{nlm}) \in [0, 2\pi]$]. For the luminosity distance d_L, we use uniform priors bounded by the 95% credible interval of the posterior distribution reported by the LIGO-Virgo-KAGRA Collaborations. The luminosity distance d_L is converted to redshift assuming a ΛCDM cosmology, with $H_0 = 67.9\ \mathrm{km\,s^{-1}\,Mpc^{-1}}$ the Planck 2015 value of the Hubble constant [47]. The prior on the coupling length scale is taken to be uniform in $\ell \in [0, 500]$ km. To maintain consistency with the perturbative small-coupling treatment, we exclude parameter regions corresponding to $\zeta > 1$. We also discard parameter combinations yielding $\mathrm{Im}(\omega) \geq 0$, which lie outside the validity regime of the damped-ringdown model adopted here. Posterior sampling is performed using 4096 live points, and posterior distributions are reconstructed using kernel density estimation. Additional robustness studies examining the dependence on the ringdown start time, astrophysical priors, and small-coupling assumptions are presented in the Supplemental Material [26].

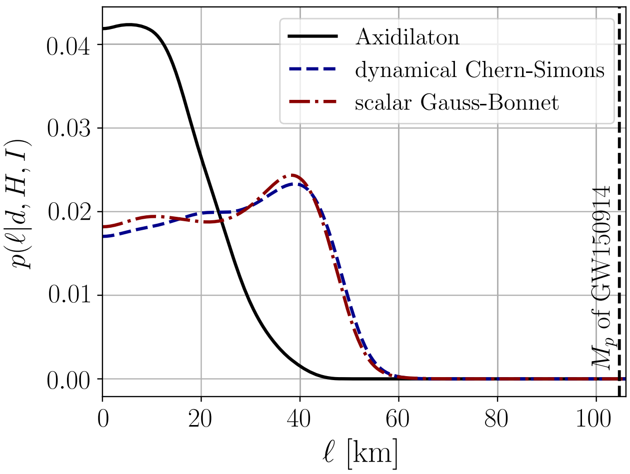

FIG. 1. Combined marginalized posterior distribution of the coupling length scale, ℓ (in km), for scalar fields in axidilaton (solid black), dynamical Chern-Simons (dashed blue) and scalar Gauss-Bonnet (dashed-dotted red) effective theories, obtained by performing Bayesian inference of the ringdown part of the signal whose signal-to-noise ratio ≥ 25. The vertical line indicates the maximum allowed $\ell \coloneqq M_{\rm map}$ within the small-coupling approximation for the corresponding signal, where $M_{\rm map}$ is the maximal-posterior remnant mass (in km) of the GW150914 event (the least massive of the events for our analysis) in the source frame inferred assuming $\ell = 0$.

Results. Figure 1 shows the combined marginalized posterior distribution [cf. Eq. (7)] of the coupling length scale, ℓ (in km), for (pseudo)scalar fields with the axidilaton (solid black), dynamical Chern-Simons (dashed blue) and scalar Gauss-Bonnet (dashed-dotted red) couplings, obtained by performing Bayesian inference of the ringdown signals of the selected events. The vertical line indicates the maximal-posterior remnant mass (in km) of the GW150914 event (the least massive of the events for our analysis) in the source frame inferred assuming $\ell = 0$, which represents the longest coupling length scale within which the small-coupling approximation is valid. We find that all posteriors are consistent with $\ell = 0$, with no evidence for the presence of (pseudo)scalar fields. Using Eq. (8), we find that the corresponding 90% credible upper limits are $\ell \lesssim 25.9$, 45.2, and 44.4 km for the axidilaton, dynamical Chern-Simons, and scalar Gauss-Bonnet couplings, respectively. Results from individual events are shown in Fig. 1 (in Supplemental Material [26]) and Table I. Most of the posterior support corresponds to $\zeta \lesssim 10^{-2}$, supporting the leading-order treatment adopted in the waveform model, including the omission of scalar-led quasinormal modes and higher-order spectral corrections. A large number of robustness tests are also presented in Supplemental Material [26].

Observe that the posteriors for ℓ for fields with axidilaton coupling are the most narrow, with a tighter 90% credible upper limit, compared to the other quadratic-gravity theories. This feature is reasonable because the shift of the quasinormal-mode frequencies with axidilaton coupling is the sum of that in dynamical Chern-Simons and scalar Gauss-Bonnet couplings. In the former, axial quasinormal-mode spectra are more significantly modified, while in the latter, stronger modifications appear in the polar spectra. Consequently, axidilaton coupling modifies both parity sectors manifestly, making it an easier theory to rule out and leading to the most stringent constraints on ℓ.

We have verified that our results are robust and consistent with the assumptions underlying our analysis. First, we have confirmed that all posterior samples satisfy $\zeta \ll 1$, ensuring that the small-coupling approximation remains valid. We have also verified that our constraints on ℓ are not artifacts of excluding $\zeta \geq 1$ or $\mathrm{Im}(\omega) > 0$ from the priors. The width of the ℓ posteriors of the field with dynamical Chern-Simons coupling agrees with previous estimates [22], further supporting the validity of our inference. We also find no significant degeneracy between ℓ and the remnant black hole's mass and spin (i.e., a waveform with nonzero ℓ cannot mimic a general-relativity waveform with different M_z and a). Additionally, we have confirmed that relaxing the approximation $A^{-,(\mathrm{P})}_{nlm} = (-1)^l (A^{+,(\mathrm{P})}_{nlm})^\dagger$ and including an overtone do not significantly affect the constraints. Finally, we have checked that our results are robust against numerical errors in the quasinormal-mode computations, systematic errors in the quasinormal-mode spectra model for spins $a > 0.75$, and the choice of ringdown start time, provided that merger nonlinearities have sufficiently subsided. In particular, the joint posteriors place the vast majority of support within the region $a \lesssim 0.75$, i.e., within the calibrated spin range of the quasinormal-mode spectra used

TABLE I. The 90% credible upper limits on ℓ (in km), as defined in Eq. (8), for various couplings. The constraints are obtained by individually analyzing the ringdown signals selected according to the two criteria stated in the main text, as well as from their combined posterior.

Events	Axidilaton (AD)	Dynamical Chern-Simons (dCS)	Scalar Gauss-Bonnet (sGB)
GW150914	40.0	53.9	57.8
GW190521_074359	57.5	78.0	86.9
GW200129_065458	44.6	62.1	70.2
GW231226_101520	42.3	59.9	74.5
GW250114_082203	35.5	48.1	50.6
Combined	25.9	45.2	44.4

here. We also verified that the small-coupling expansion parameter ϵ remains well below unity for the posterior mass, and that the inferred limits are insensitive to reasonable variations of (i) the treatment of $\mathrm{Im}(\omega)$ cutoffs, (ii) numerical uncertainties in the parameters of the fitting expression of the quasinormal-mode frequencies, and (iii) the ringdown start time. These checks collectively ensure that the inference remains inside the domain where the underlying quasinormal-mode modeling is quantitatively reliable. Further details are provided in the Supplementary Material [26].

Our constraints on pseudo(scalar) fields differ from those in [48] by a factor of $\sim$4 because of various differences in analysis methodology. First, [48] included the inspiral, merger and ringdown phases in their analysis, but only considers effects from the pseudo(scalar) fields in the merger and ringdown phase (even though modifications to the merger are not known accurately), while we only consider the ringdown phase. Their whole-signal analysis recovers a signal-to-noise ratio of $\sim$25, whereas our ringdown-only analysis yields signal-to-noise ratios $\lesssim 7$, roughly a factor of 4 smaller. Second, their analysis uses a model for the quasinormal-mode frequency shift that is accurate only to first order in a, which is valid only when $a \lesssim 0.3$; our analysis uses the frequencies in [18,21,22] which is accurate up to $a \lesssim 0.75$ and thus applicable to black hole remnants produced in the collision of nonspinning black holes (see also Supplementary Material [26]). Third, their analysis includes only the less-damped parity sector of each field, whereas we incorporate shifts in both axial and polar quasinormal modes. Therefore, although the reported constraints in [48] are claimed to be more stringent (due to the use of a larger signal-to-noise ratio), the results presented here are more robust.

Concluding remarks. Our analysis constitutes a ringdown-based search for scalar fields that incorporates parity-dependent quasinormal-mode spectra calibrated for moderately spinning black holes, explicitly accounting for the breaking of isospectrality. We obtain the first gravitational-wave constraint on axidilaton-type coupling, together with bounds on dynamical Chern-Simons and scalar Gauss-Bonnet couplings from the ringdown components of the analysed signals. By isolating the ringdown phase, our approach reduces dependence on modeling assumptions spanning multiple dynamical regimes. A quantitative comparison with previous analyses is provided in Supplemental Material [26].

Our results demonstrate that black hole ringdown observations alone can already provide meaningful constraints on additional degrees of freedom beyond general relativity at horizon scales. In particular, the absence of detectable parity-dependent effects in the quasinormal-mode spectrum places bounds on curvature-coupled scalar fields that modify the strong-field dynamics of gravity. These constraints are complementary to those obtained from full-waveform analyses and other astrophysical probes.

Looking ahead, the sensitivity of ringdown searches will improve as the number of detected events increases. Current observations already constrain coupling length scales to values significantly below the horizon size of stellar-mass black holes, and combining multiple events will further tighten these bounds. Future developments, including improved modeling of parity-dependent quasinormal-mode spectra and extensions to inspiral-merger-ringdown analyses, will further expand the reach of black hole ringdown spectroscopy as a probe of gravity and additional fields.

Acknowledgments. The authors acknowledge the support from the Simons Foundation through Award No. 896696, the NSF through Grant No. PHY-2207650 and NASA through Grant No. 80NSSC22K0806. A. K.-W. C. also acknowledges the Herchel Smith Fellowship at the University of Cambridge for support of this work. The authors thank Emanuele Berti, Mark Cheung, Carl-Johan Haster, Kelvin K. H. Lam, Tjonnie G. F. Li, Samson H. W. Leong, Hector O Silva, Isaac C. F. Wong, and Sophia Yi for insightful discussion. A. K.-W. C. would like to thank Simon Maenaut and Gregorio Carullo for advise on preparing and sharing the configuration files for pyRing analyses. The calculations and results reported in this Letter were produced using the computational resources of the Illinois Campus Cluster, a computing resource that is operated by the Illinois Campus Cluster Program (ICCP) in conjunction with National Center for Supercomputing Applications (NCSA), and is supported by funds from the University of Illinois at Urbana-Champaign, and used Delta at NCSA through allocation PHY240142 from the Advanced Cyberinfrastructure Coordination Ecosystem: Services & Support (ACCESS) program, which is supported by National Science Foundation Grants No. 2138259, No. 2138286, No. 2138307, No. 2137603, and No. 2138296. The author would like to especially thank the investors of the IlliniComputes initiatives and GravityTheory computational nodes for permitting the authors to execute runs related to this work using the relevant computational resources. ASTROPY [49], Matplotlib [50], NumPy [51], SciPy [52], pyRing [41].

Data availability. The gravitational-wave strain data analyzed in this work are publicly available through the Gravitational Wave Open Science Center (GWOSC) at [53]. The time-domain inference package pyRing, used in this work to search for direct waves, is publicly available at [41].

[1] A. H. Guth, The inflationary universe: A possible solution to the horizon and flatness problems, Phys. Rev. D **23**, 347 (1981).

[2] J. Martin, C. Ringeval, and V. Vennin, Encyclopædia inflationaris: Opiparous edition, Phys. Dark Universe **5–6**, 75 (2014).

[3] R. Kallosh and A. Linde, Dilaton-axion inflation with PBHs and GWs, J. Cosmol. Astropart. Phys. 08 (2022) 037.

[4] K. Saaidi and A. Mohammadi, Brane cosmology with the Chameleon scalar field in bulk, Phys. Rev. D **85**, 023526 (2012).

[5] P. M. Sá, Late-time evolution of the Universe within a two-scalar-field cosmological model, Phys. Rev. D **103**, 123517 (2021).

[6] A. L. Ferreira, N. Pinto-Neto, and J. Zanelli, Inflation and late-time accelerated expansion driven by k-essence degenerate dynamics, Phys. Rev. D **109**, 023515 (2024).

[7] Stephon H. S. Alexander, M. E. Peskin, and M. M. Sheikh-Jabbari, Leptogenesis from gravity waves in models of inflation, Phys. Rev. Lett. **96**, 081301 (2006).

[8] S. Alexander and N. Yunes, Chern-Simons modified general relativity, Phys. Rep. **480**, 1 (2009).

[9] A. J. Shajib and J. A. Frieman, Scalar-field dark energy models: Current and forecast constraints, Phys. Rev. D **112**, 063508 (2025).

[10] P. A. Cano and A. Ruipérez, Leading higher-derivative corrections to Kerr geometry, J. High Energy Phys. 05 (2019) 189.

[11] K. K.-H. Lam, A. K.-W. Chung, and N. Yunes, Spinning black holes in modified gravity via spectral methods, Phys. Rev. Lett. **136**, 021401 (2026).

[12] K. K.-H. Lam, A. K.-W. Chung, and N. Yunes, Analytic and accurate approximate metrics for black holes with arbitrary rotation in beyond-Einstein gravity using spectral methods, Phys. Rev. D **113**, 024030 (2026).

[13] A. Maselli, N. Franchini, L. Gualtieri, T. P. Sotiriou, S. Barsanti, and P. Pani, Detecting fundamental fields with LISA observations of gravitational waves from extreme mass-ratio inspirals, Nat. Astron. **6**, 464 (2022).

[14] S. Barsanti, A. Maselli, T. P. Sotiriou, and L. Gualtieri, Detecting massive scalar fields with extreme mass-ratio inspirals, Phys. Rev. Lett. **131**, 051401 (2023).

[15] A. Maselli, N. Franchini, L. Gualtieri, and T. P. Sotiriou, Detecting scalar fields with extreme mass ratio inspirals, Phys. Rev. Lett. **125**, 141101 (2020).

[16] J. C. Aurrekoetxea, K. Clough, J. Bamber, and P. G. Ferreira, Effect of wave dark matter on equal mass black hole mergers, Phys. Rev. Lett. **132**, 211401 (2024).

[17] S. Roy, R. Vicente, J. C. Aurrekoetxea, K. Clough, and P. G. Ferreira, Scalar fields around black hole binaries in LIGO-Virgo-KAGRA, Phys. Rev. Lett. **136**, 191402 (2026).

[18] A. K.-W. Chung and N. Yunes, Quasinormal mode frequencies and gravitational perturbations of black holes with any subextremal spin in modified gravity through METRICS: The scalar-Gauss-Bonnet gravity case, Phys. Rev. D **110**, 064019 (2024).

[19] E. Berti *et al.*, Black hole spectroscopy: From theory to experiment, arXiv:2505.23895.

[20] A. K.-W. Chung, P. Wagle, and N. Yunes, Spectral method for metric perturbations of black holes: Kerr background case in general relativity, Phys. Rev. D **109**, 044072 (2024).

[21] A. K.-W. Chung and N. Yunes, Ringing out general relativity: Quasinormal mode frequencies for black holes of any spin in modified gravity, Phys. Rev. Lett. **133**, 181401 (2024).

[22] A. K.-W. Chung, K. K.-H. Lam, and N. Yunes, Quasinormal mode frequencies and gravitational perturbations of spinning black holes in modified gravity through METRICS: The dynamical Chern-Simons gravity case, Phys. Rev. D **111**, 124052 (2025).

[23] S. H. S. Alexander and S. J. Gates, Jr., Can the string scale be related to the cosmic baryon asymmetry?, J. Cosmol. Astropart. Phys. 06 (2006) 018.

[24] D. J. Gross and E. Witten, Superstring modifications of Einstein's equations, Nucl. Phys. **B277**, 1 (1986).

[25] D. J. Gross, J. A. Harvey, E. J. Martinec, and R. Rohm, Heterotic string theory. 2. The interacting heterotic string, Nucl. Phys. **B267**, 75 (1986).

[26] See Supplemental Material at http://link.aps.org/supplemental/10.1103/2ctd-mgb6 for further details of the (pseudo) scalar fields, the derivation of Eq. (2), and the results of the sanity checks.

[27] R. D. Blandford and R. L. Znajek, Electromagnetic extractions of energy from Kerr black holes, Mon. Not. R. Astron. Soc. **179**, 433 (1977).

[28] W. Israel, Event horizons in static electrovac space-times, Commun. Math. Phys. **8**, 245 (1968).

[29] S. Maenaut, G. Carullo, P. A. Cano, A. Liu, V. Cardoso, T. Hertog, and T. G. F. Li, Ringdown analysis of rotating black holes in effective field theory extensions of general relativity, Phys. Rev. D **113**, 044039 (2026).

[30] A. G. Abac *et al.* (LIGO Scientific Collaboration, VIRGO Collaboration, and KAGRA Collaboration), GWTC-4.0: Tests of general relativity. III. Tests of the remnants, arXiv:2603.19021.

[31] B. P. Abbott *et al.* (LIGO Scientific Collaboration and Virgo Collaboration), GWTC-1: A gravitational-wave transient catalog of compact binary mergers observed by LIGO and Virgo during the first and second observing runs, Phys. Rev. X **9**, 031040 (2019).

[32] R. Abbott *et al.* (LIGO Scientific Collaboration and Virgo Collaboration), GWTC-2: Compact binary coalescences observed by LIGO and Virgo during the first half of the third observing run, arXiv:2010.14527.

[33] R. Abbott *et al.* (LIGO Scientific Collaboration, VIRGO Collaboration, and KAGRA Collaboration), GWTC-3: Compact binary coalescences observed by LIGO and Virgo during the second part of the third observing run, Phys. Rev. X **13**, 041039 (2023).

[34] B. P. Abbott *et al.* (LIGO Scientific Collaboration and Virgo Collaboration), Tests of general relativity with the binary black hole signals from the LIGO-Virgo catalog GWTC-1, Phys. Rev. D **100**, 104036 (2019).

[35] R. Abbott *et al.* (LIGO Scientific Collaboration and Virgo Collaboration), Tests of general relativity with binary black holes from the second LIGO-Virgo gravitational-wave transient catalog, Phys. Rev. D **103**, 122002 (2021).

[36] R. Abbott *et al.* (LIGO Scientific Collaboration, VIRGO Collaboration, and KAGRA Collaboration), Tests of general relativity with GWTC-3, Phys. Rev. D **112**, 084080 (2025).

[37] R. Abbott *et al.* (LIGO Scientific Collaboration and Virgo Collaboration), GWTC-2: Compact binary coalescences observed by LIGO and Virgo during the first half of the third observing run, Phys. Rev. X **11**, 021053 (2021).
[38] A. G. Abac *et al.* (LIGO Scientific Collaboration, Virgo Collaboration, and KAGRA Collaboration), Black hole spectroscopy and tests of general relativity with GW250114, Phys. Rev. Lett. **136**, 041403 (2026).
[39] M. Isi, M. Giesler, W. M. Farr, M. A. Scheel, and S. A. Teukolsky, Testing the no-hair theorem with GW150914, Phys. Rev. Lett. **123**, 111102 (2019).
[40] M. Isi and W. M. Farr, Comment on “Analysis of Ringdown Overtones in GW150914”, Phys. Rev. Lett. **131**, 169001 (2023).
[41] G. Carullo, W. Del Pozzo, and J. Veitch, “pyRing: A time-domain ringdown analysis Python package,” https://git.ligo.org/lscsoft/pyring (2023).
[42] G. Carullo *et al.*, Empirical tests of the black hole no-hair conjecture using gravitational-wave observations, Phys. Rev. D **98**, 104020 (2018).
[43] G. Carullo, G. Riemenschneider, K. W. Tsang, A. Nagar, and W. Del Pozzo, GW150914 peak frequency: A novel consistency test of strong-field general relativity, Classical Quantum Gravity **36**, 105009 (2019).
[44] G. Carullo, W. Del Pozzo, and J. Veitch, Observational black hole spectroscopy: A time-domain multimode analysis of GW150914, Phys. Rev. D **99**, 123029 (2019); **100**, 089903 (E) (2019).
[45] M. H.-Y. Cheung *et al.*, Nonlinear effects in black hole ringdown, Phys. Rev. Lett. **130**, 081401 (2023).
[46] K. Mitman *et al.*, Nonlinearities in black hole ringdowns, Phys. Rev. Lett. **130**, 081402 (2023).
[47] P. A. R. Ade *et al.* (Planck Collaboration), Planck 2015 results. XIII. Cosmological parameters, Astron. Astrophys. **594**, A13 (2016).
[48] H. O. Silva, A. Ghosh, and A. Buonanno, Black-hole ringdown as a probe of higher-curvature gravity theories, Phys. Rev. D **107**, 044030 (2023).
[49] Astropy Collaboration *et al.*, The astropy project: Sustaining and growing a community-oriented open-source project and the latest major release (v5.0) of the core package, Astrophys. J. **935**, 167 (2022).
[50] J. D. Hunter, Matplotlib: A 2D graphics environment, Comput. Sci. Eng. **9**, 90 (2007).
[51] C. R. Harris *et al.*, Array programming with NumPy, Nature (London) **585**, 357 (2020).
[52] P. Virtanen *et al.*, SciPy 1.0: Fundamental algorithms for scientific computing in Python, Nat. Methods **17**, 261 (2020).
[53] https://gwosc.org/eventapi/.